soil derived dust emissions from arid areas: compared results from IR-channel satellite observation and by means of simulations

Michel Legrand, Claude N'Doumé, Beatrice Marticorena, Gilles Bergametti, Yann Callot

Soil-derived dust emission from arid areas: Compared results from IR-channel satellite observation and by means of simulations

Michel Legrand and Claude N'doumé

Laboratoire d'Optique Atmosphérique, Université de Lille-1, F-59655 Villeneuve d'Ascq cedex, France

Béatrice Marticorena and Gilles Bergametti

Laboratoire Interuniversitaire des Systèmes Atmosphériques, URA CNRS 1404, Universités de Paris 7 & 12, Centre Multidisciplinaire de Créteil, 61 Av. du Gal de Gaulle, F-94010 Créteil cedex, France

Yann Callot

URBAMA, Université de Tours, Site Loire, BP 1028, F-37012 Tours cedex, France

ABSTRACT

This article deals with a comparison between dust fluxes simulated with a physical emission scheme and satellite observations of desert dust emissions. This physical scheme allows to quantify the dust emissions as a function of the parameters describing the surface characteristics in the source-region: soil nature (size-distribution and mineralogy) and surface roughness. The surface properties of the western Sahara have been mapped on a grid (1°×1°), using a geomorphologic approach, in order to determine the soil parameters required to perform large-scale simulations of dust emissions. The surface wind velocities are supplied by the analyses of the European Centre for Medium Range Weather Forecast (ECMWF). The western Sahara proves to be strongly non-uniform as to the threshold velocities and the related dust emissions. The spatio-temporal distributions of the emitted dust simulated by the model and the Infrared Difference Dust Index (IDDI) derived from Meteosat observations reveal a close agreement, far from being reached when using the currently used single threshold source-functions. A quantitative relation is observed for the emission strength, in the form of a linear fit between the IDDI and the logarithm of the mass flux simulated by the dust production scheme.

1. INTRODUCTION

The global production of total aerosol is estimated to be 3.5 billion tons a year[1]. Over 50% of this amount is made up of mineral aerosol, also called desert aerosol or dust, since it originates mainly from the deserts and their borders. This atmospheric dust widely interacts with the climate. The emission strength and location are sensitive to wind and precipitation changes. Several studies on the paleoclimate have unambiguously shown the sensitivity of the response of dust emission to climatic changes[2,3,4]. This is also observed over shorter periods as reported in studies related to the droughts episodes that stroke the Sahel since the 70s[5,6]. In turn, the atmospheric content is affected by the changes in emission, producing significant effects on the radiative budget and on the physics and chemistry of clouds. So the mineral aerosol is a topic of noticeable interest within the scope of climate change, on a global scale as well as in those regions particularly concerned by its presence. Although this fact has been evident for many years, the efforts of the modelists to properly depict the dust distribution have not been entirely successful so far[7,8,9]. A major reason for this is to be searched in the incomplete description of the emission processes and the poor documentation on the ground surface and soil characteristics of the arid areas, leading to questionable locations for the dust sources[7].

In order to cope with these appreciable difficulties, a physical scheme dedicated to dust emission from arid areas has been designed[10]. For supplying the requisite input data for the scheme application on a large scale, a description of the surface roughness features and the soil nature has been brought about on a geomorphologic basis, and a cartography of the relevant parameters has been derived over an area covering the western half of the Sahara. Then, using meteorological wind fields, the scheme simulates dust emissions. In situ validations of such simulated emissions could hardly be conceived. Instead, remote sensing of dust over the Sahara is regularly performed with satellite data and constitutes an adequate mean of control and validation, easy to implement. A technique applied to the IR images of Meteosat results in imaging the Infrared Difference Dust Index (IDDI). Analyses carried out using this parameter have resulted in an improved location of the major Saharan sources along with a description of their seasonal cycle of activity[11,12]. In this paper, the satellite-observed emitted dust supplied by the IDDI is utilized for the validation of the dust emission fluxes simulated by application of the scheme to the western Saharan surfaces for the year 1991.

0-8194-1942-7/95/$6.00

2. DUST EMISSION SCHEME

In order to represent correctly the spatial and temporal variability of dust emission in arid environment, a physical explicit scheme, applicable on a large scale, has been designed[10], whose bases are briefly described hereafter.

The arid surfaces are represented by two components: (i) an erodible surface covered with loose grains - individual particles and aggregates - with a diameter D_p in the submillimetric range, and (ii) "steady" obstacles constituting roughness elements such as gravel, pebbles, stones, plants and so on. The aeolian friction on this surface means a transfer of momentum and kinetic energy from the atmosphere to the surface. This process is characterized by the wind shear stress τ or alternatively by the wind friction velocity U*:

$$\tau = \rho_a U^{*2} \tag{1}$$

where ρ_a is the air density. The wind friction velocity is a function of the wind velocity and of the surface roughness. Due to their weight and the forces of cohesion acting between the particles at rest, the value of U* needs to reach a threshold depending on the particles size[13] $u^*_t(D_p)$ for the motion of these particles to be initiated over a smooth surface (i.e. without obstacle). In the presence of obstacles, the aeolian shear stress is shared between the obstacles and the erodible soil[14,15,16]. A drag partition scheme has been developed to quantify an effective friction velocity ratio $f(Z_0,z_0)$ and a related increased threshold $U^*_t(D_p,Z_0,z_0)$, as a function of the roughness length produced by the obstacles Z_0, and of the roughness length of the erodible part of the surface z_0:

$$U^*_t(D_p,Z_0,z_0) = \frac{u^*_t(D_p)}{f(Z_0,z_0)} \tag{2}$$

Once the wind velocity reaches this threshold value, a saltation regime settles in a shallow layer some tens centimeters deep. In this process, the collisions of the grains falling down onto the surface, release the fine particles generally included in the aggregates[17]. These fine particles are then set in suspension over the saltation layer, constituting the dust clouds carried away by the wind.

Including the previous expression of the threshold wind friction velocity in a theoretical formulation of the horizontal flux[18], experimentally tested[18,19], provides a size-dependent parameterization of the horizontal flux. Thus, the total flux in the saltation layer G is obtained by integrating the contributions of the various sizes of erodible grains:

$$G = KrU^{*3} \int_{D_p} [1+\frac{U^*_t}{U^*}][1-\frac{U^{*2}_t}{U^{*2}}] dS_{rel}(D_p) dD_p \tag{3}$$

the quantities in brackets depending upon D_p via U^*_t, and

$K = \rho_a/g$, g being the gravitational acceleration,

r is the ratio of erodible to total surface,

dS_{rel} is the normalized basal (i.e. "covered") area for the particles with a size within $[D_p,D_p+dD_p]$, relative to the erodible area; this quantity contains the information on the (loose) grain size distribution in the soil, described with respect to the mass by a log-normal distribution, $dM(D_p)/dLnD_p$.

At last, to quantify the vertical flux F of fine particle (or aerosol) generated during the saltation, an empirical relation based on coupled measurements of F and G performed on various arid soils[20], has been established between the ratio of vertical to horizontal flux F/G and the soil clay content α:

$$Log(F/G) = a\alpha+b \tag{4}$$

this relation being no longer valid for crusted soils where the clay content is greater than 50%.

The consistency of this dust emission model has been established, by validating the various steps of the physical scheme with results of experiments reported in the relevant literature[20,21,22,23,24].

3. SCHEME APPLICATION ON A LARGE SCALE

The dust emission scheme being established, it can be used on large scale to perform dust emission simulations if the required input parameters: U^*, Z_0, z_0, r, $dM/dLnD_p$ and α, are provided. Specific methods[25] have been developed to determine these parameters from data accessible on a large scale.

1) In adiabatic conditions, the wind friction velocity U^* is related to the wind speed at height Z by[26]

$$U(Z) = \frac{U^*}{\kappa} Ln\left(\frac{Z}{Z_0}\right) \tag{5}$$

where κ is the Kármán constant. So the adiabatic hypothesis being assumed and the roughness length Z_0 being known, U^* can be computed from the wind speed U at height Z. An additional roughness must be accounted for in the case of soil movement. Indeed, the soil particles in the saltation layer behave like obstacles and thus produce a "saltation roughness", increasing with the wind friction velocity. This saltation roughness length is parameterized as a function of the initial surface roughness length Z_0, and of the square of the wind friction velocity[27]. The wind fields are provided by the European Centre for Medium Range Weather Forecast (ECMWF). The surface values, i.e. at a level 10-m high, have been used to avoid the effect of the large-scale topography on roughness. The data at 1200 UTC for the year 1991 have been used over the region of concern [16°N-36°N, 17°W-12°E] with a resolution (1°×1°).

2) The roughness length Z_0 is derived from an empirical relation established between the roughness density λ and the ratio of roughness length to mean height h of the non-erodible elements, based on wind-tunnel measurements. Additional hypotheses about the shape of the non-erodible elements allow to estimate the roughness length Z_0 and the fraction of erodible surface r from the roughness covering rate and the mean height of the non erodible elements. So, a cartography of the nature, mean height and covering rate of the obstacles has been performed, with a resolution (1°×1°). This was implemented through a geomorphologic approach resulting in a qualitative description of the landscape and ultimately calibrated using "ground truths". The manifold field investigations performed by Y. Callot[28,29] in the region of concern offered the opportunity for supplying these ground truths and thus applying this strategy. As a result every element (1°×1°) has been characterized with fractions of (up to five) surface types defined according to the kinds of roughness element (inert obstacles or vegetation) and the classes for height h and relative covering rate of the obstacles (1-r).

3) The parameters related to the erodible soil are the "smooth" roughness length z_0, the mass size distribution $dM(D_p)/dLnD_p$ and the clay content α. These parameters are determined from a mineralogical description of the soil coupled with a simple representation method of the soil from arid regions[30]. This representation has been established from a set of 26 samples of soils collected at various sites in arid and semi-arid regions (Sahara, California and Spain), which has been analysed using dry sieving and chemical analysis. From these analyses, it was found that all the samples can be represented as a mixture in various proportions of four typical populations. These four populations have been characterized both from a granulometric ($dM(D_p)/dLnD_p$) and mineralogical point of view (alumino-silicated silt, fine quartz sand, coarse dune sand, salty soil). Wet sedimentation technique applied to five selected soil samples allowed to estimate the clay content of these four populations, and to assign them a specific ratio of vertical to horizontal flux. Thus a mineralogical description, in the form of a mixture of the four reference mineralogical populations, allows to assign any soil its own values for $dM(D_p)/dLnD_p$, z_0, and the ratio F/G. The soil types resulting from this representation have been mapped together with the roughness types.

For the sake of illustration of the effect of the surface characteristics, Fig. 1 shows the map of wind velocities for erosion threshold, defined at a height of 10-m, in the western part of the Sahara. Since it depends on the steady surface characteristics, this essential parameter is assumed to be time-independent. Apart from completely non-erodible elements (in white) representing mountains and ocean, the threshold is highly variable, ranging from 6.5 ms^{-1} to 20 ms^{-1}, these values being in agreement with the field measurements of threshold wind velocity reported in the literature. This pattern lets predict a strong heterogeneity of both the intensity and the location of the dust emissions, backing up the concept of well-delimited source areas.

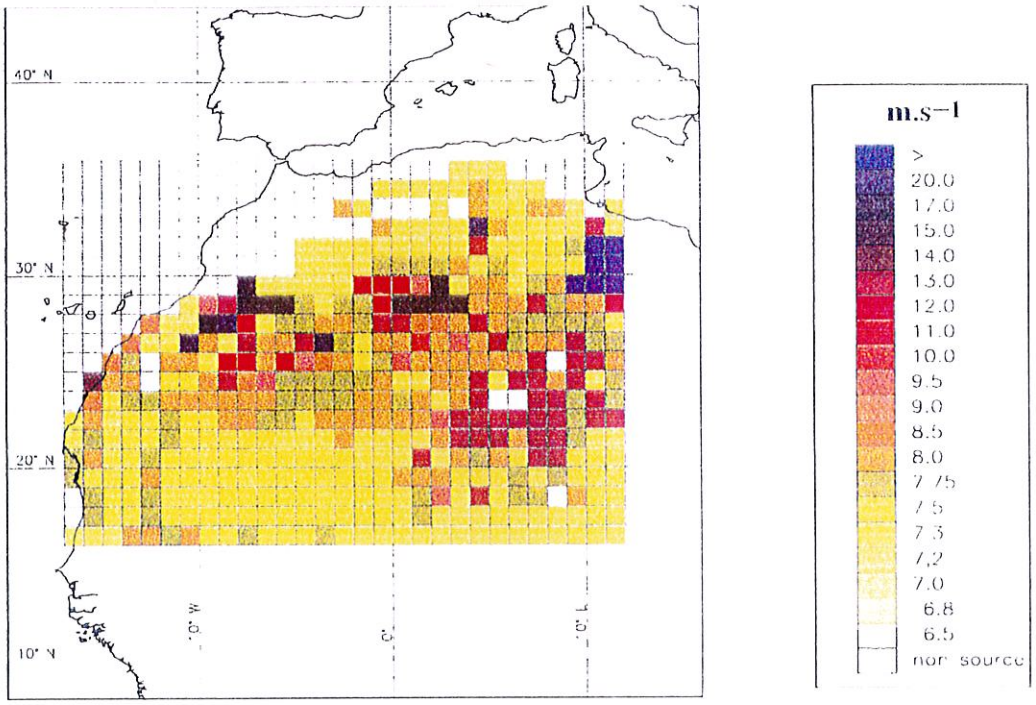

Fig. 1 Distribution of the wind velocity for erosion threshold defined at a height of 10-m, with a resolution of a square degree over the western Sahara

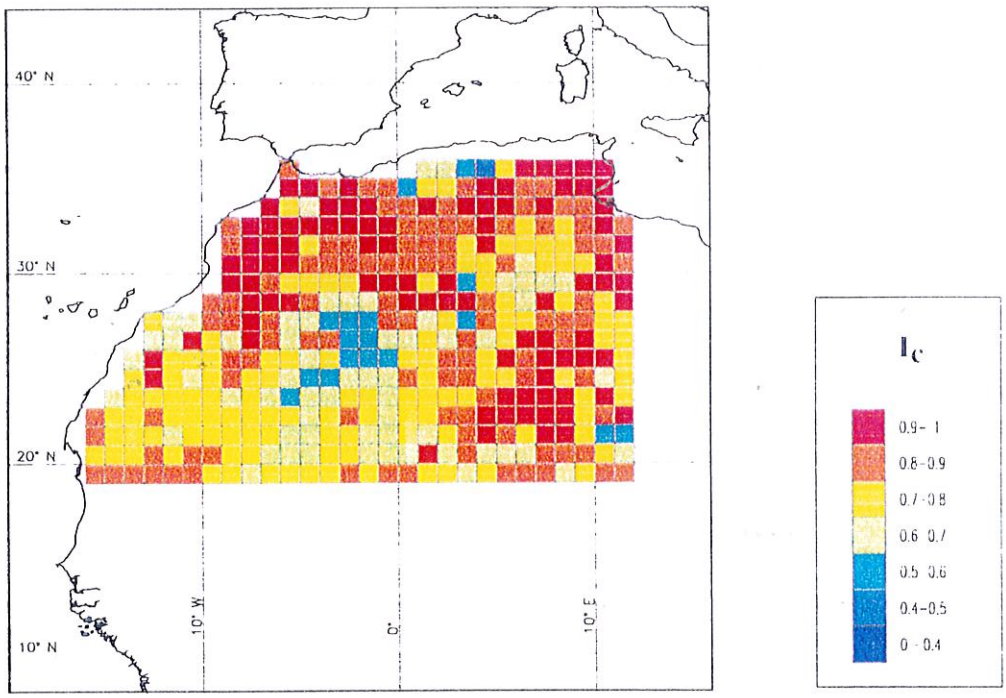

Fig. 2 Distribution of the confidence index depicting the consistency between dust emission simulated with the dust production model and observed by the satellite Meteosat, with a resolution of a square degree throughout the western Sahara. The confidence index integrates daily comparison over five months of 1991.

4. EMITTED DUST OBSERVED FROM SATELLITE

The dust emitted by the Saharan sources and transported by the prevailing winds can be observed by means of the IR images of Meteosat. During daytime, it can be tracked further over the ocean with the VIS images from the same satellite. The IR parameter permitting this observation during daytime - the IDDI whose extraction has been described in previous articles[12] - can be defined as the radiance decrease in the [10.5-12.5μm] range (IR-channel of Meteosat) resulting from the presence of dust.

Experimental case studies of compared variations of the IDDI (labelled c hereafter) with the aerosol optical depth δ (in the visible or near IR range) based on time series of photometric measurements have given rise to empirical linear or quasi-linear relations between these parameters[31,32]:

$$c = a\delta\ (+\ \varepsilon\delta^2)\ \ (\varepsilon \text{ small}) \tag{6}$$

The comparison between c and δ according to a statistical procedure applied to routine observations of visibility range collected in 39 African stations throughout one year, has resulted in a relation resembling to (6). For a sake of simplicity, c and δ can be considered as directly proportional:

$$c = A\delta \tag{7}$$

with a value of about 15-20 cts for A (i.e. a unit dust optical depth results in 15-20 cts of IDDI, on a statistical basis).

Since δ is proportional to the dust amount in a vertical column, it can be inferred that the IDDI is also proportional to this dust amount. But this simple logic is also ambiguous. Indeed it must be stated that this law holds for the dust amount and IDDI of a specified dust model - i.e. with prescribed particle size distribution and complex refractive index. Hence, should the dust have been very variable with respect to its microphysical and optical properties during the periods of the photometric measurements used in the reported case studies, the relations (6) could not have been obtained. As for the relation (7), it has been established and it holds only as a statistical average. This view is confirmed by simulations of the response of Meteosat[33,34] to the dust impact (i.e. simulations of IDDI): (i) the variations of c are quasi-linear as a function of δ, and so as a function of the mass M of dust load in the vertical column; (ii) dust models distinct as to their size distribution associated with identical values of δ provide different values of c; (iii) with a given value of δ, c increases with M. This latter result is crucial. It is due to the fact that the increase of M according to the dust model relates to the predominance in large particles and hence to an increase of c (via the increase of the IR dust optical depth). So it can be expected that the IDDI is suitable for mass loading estimates, albeit no elaborate study has been engaged on this question so far.

5. COMPARISON OF OBSERVED AND SIMULATED EMITTED DUST

5.1 Comparing the occurrence of dust emissions

The comparisons have been carried out at a spatial resolution (1°×1°) for an area extending from 36°N to 16°N and 17°W to 12°E.

At the outset, it must be noted that the satellite data include indistinctly dust emitted during the satellite image take, and transported dust emitted further back, sometimes several days ago. Thus, the simulated dust emissions fluxes, which are instant values, are not directly comparable to the IDDI. Since the largest emitted particles sediment rapidly, and diffusion operates in the dust layer, it is reasonable to assume that the highest values of the IDDI mainly correspond to emissions. Therefore, a high threshold of IDDI has been selected to sort out as much as possible the situations of dust transport from the situations of dust emission. An IDDI threshold of 30 cts has been selected, corresponding to 2.4 $W.m^{-2}.sr^{-1}$ of radiance decrease in the IR-channel of Meteosat-4, and about 15 K in brightness temperature drop. According to equation (7) such a dust amount corresponds statistically to an optical depth of about 1.5-2.

When using a high IDDI threshold, the cases of weak satellite-observed dust content (< 30 cts) are separated, even if they correspond to low emissions. Therefore, a comparable threshold must be associated to the simulated fluxes of emitted dust, to separate the lowest emission fluxes, in order to compare only the intense observed dust events, to significant simulated dust fluxes. Since no relation is available between the IDDI and dust mass, the threshold has been fixed to a value of 10^{-10} $g.cm^{-2}.s^{-1}$, to be consistent with the low limit of dust content observed during dust events.

The frequencies of dust events simulated by the model and those observed by satellite have been compared by applying this couple of stated thresholds. The agreement is quantified by a confidence index I_C, defined as the ratio of coinciding cases - i.e. cases where dust emission is observed, or not, from both modeling and satellite - to the overall number of considered cases. It can be written out, using a usual logical operator:

$$I_C = \frac{N\{E(simu).and.E(obs)\} + N\{nE(simu).and.nE(obs)\}}{N_T} \quad (8)$$

where E and nE mean respectively the sets of cases with and without emission (from either simulations or observations) and N_T is the total number of cases. A full agreement means $I_C = 1$, while $I_C = 0.5$ means no statistical consistence.

Of course the cloudy cases have been picked out of the statistics since satellite observation is then prohibited. Therefore, the (1°×1°) areas are considered cloudy if over 50% of the constituting satellite pixels are identified as cloudy. Else the areas are considered clear, and they are classified as dust emitting if over 50% of the clear pixels have a value of IDDI exceeding the threshold of 30 cts (else they are classified as non emitting).

In addition, cases with a wind speed inferior to the lowest wind threshold velocity reported in the literature (4 $m.s^{-1}$) have been rejected a priori as non significant. Indeed, it is trivial for the model to simulate no dust production when the wind velocity is so low. It must be noted that this additional criterion leads to reject less than 10% of the cases previously selected for the comparison (i.e. cases where IDDI>30cts, $F>10^{-10}$ $g.cm^{-2}.s^{-1}$), except in the southernmost part of the studied area, at latitude below 20°N. This results probably from the presence of the Inter Tropical Convergence Zone, where increasing thickness of dust can be experienced in the absence of wind. Therefore, the latitude below 20°N have not been considered in this study.

In order to sample suitably the yearly changes of location and strength[11] of the Saharan dust emissions, the statistical confidence index have been computed for the months of January, March, May, July and November of 1991, totalling 22,904 tested cases.

Figure 2 presents the mapping of the confidence index, averaged over the five months of the study. Summing up over the whole studied area the averaged contribution of the (1°×1°) grid mesh results in an overall averaged confidence index of 0.79.

To provide a quantitative appreciation of these results, they have been compared to the ones obtained when applying a simple source-function with a single threshold wind velocity, such as the one used in the most recent desert dust cycle simulation [9]:

$$F \propto U^3 \left(1 - \frac{U_t}{U}\right) \quad (9)$$

where U is the wind velocity at 10 m height and $U_t = 6.5$ $m.s^{-1}$ is the threshold wind velocity at the same level.

For the comparison with the studied emission model to be significant, dust emissions have been simulated with this source-function, and analyzed together with the satellite data by following exactly the procedure previously specified for the validation of the scheme.

Figure 3 represents the frequencies of occurrence of the local confidence index averaged over the five months, for the physical scheme and for the source-function (9). The confidence index obtained with this latter function are uniformly lower, and the confidence index averaged over the five months of the study and the area of concern is 0.60 (i.e. a drop of 0.19 relatively to the previous scheme).

5.2 Comparing emitted mass fluxes and the Infrared Difference Dust Index

In a further step, the consistency between the simulated mass fluxes of emitted dust and the emissions observed by satellite has been quantitatively checked. A period of intense dust emissions has been selected for this evaluation, and only the cases where the simulated emissions fluxes were higher than the dust background level observed in source-regions, have been considered. From the literature, this background level has been estimated at a value of 10^{-11} $g.cm^{-2}.s^{-1}$. By this way, 1257 cases were retained for May 1991. For IDDI ranging from 0 to 50 cts, in the geometrical means and standard deviations of the simulated fluxes have been computed, using IDDI classes 5 ct wide. The number of tested cases varies from 68 to 238 for the various classes, except for the range 46-50, composed of 15 cases.

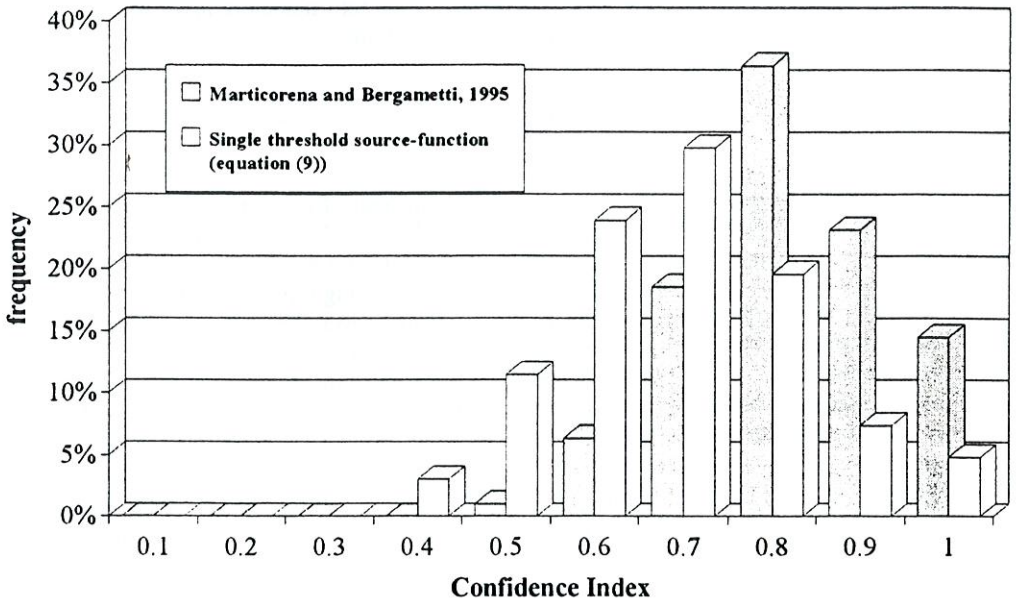

Fig. 3 Frequency distributions of the daily confidence index of the (1°×1°) area throughout the western Sahara over five months of 1991 obtained with the physical dust production scheme and with a single threshold source-function (equation 9).

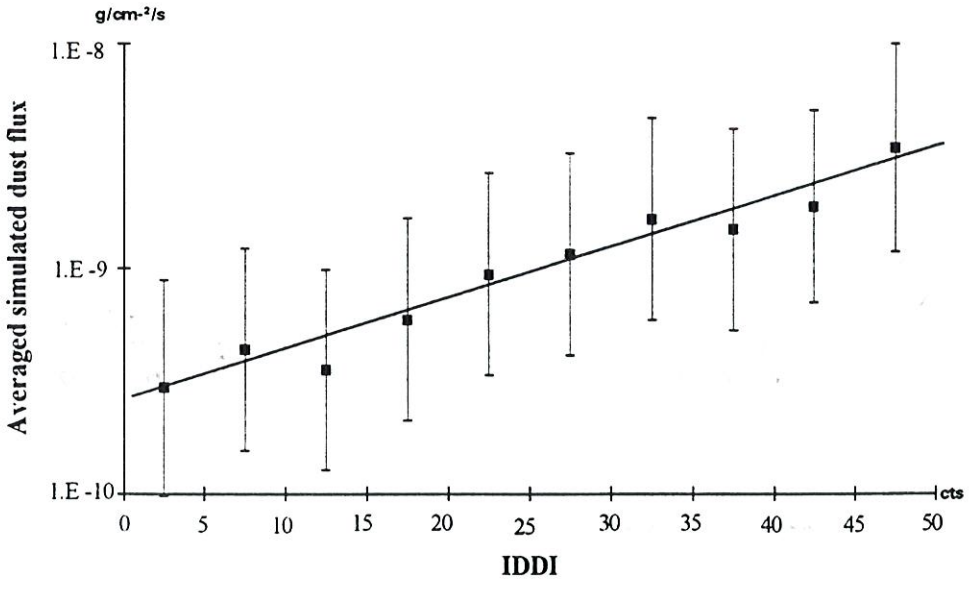

Fig. 4 Geometric mean of the simulated emitted dust flux values higher than 10^{-11} g.cm^{-2}.s^{-1} for classes IDDI 5 cts width (May 1991, western Sahara); error bars: $(\pm 2\sigma)$; linear regression: Log F = 0.0226 c - 9.61; squared correlation coefficient: r^2=0.975.

As illustrated on fig. 4, a linear relationship was observed between the logarithm of the simulated fluxes and the IDDI, with a high correlation coefficient.

$$\text{Log } F = 0.0226\ c - 9.61 \tag{10}$$

The errors bars representing $(\pm 2\sigma)$, define intervals encompassing 95 % of the initial individual data, and the squared correlation is satisfying.

6. CONCLUSION

The dust production model[10] used for the simulation of dust emissions from arid surfaces, associated with a mapping of the relevant surface characteristics for the Western Sahara, gives rise to strongly non-uniform distribution of threshold wind friction velocity and dust production. The comparison of the simulated mass fluxes, using the surface wind velocity from the ECMWF, with the dust emissions observed from Meteosat in the form of IDDI, demonstrates the ability of this scheme to supply an accurate description of the dust emissions according to time and space. By far, this accuracy in the description is not reached by application of a simple source function characterized by a single threshold wind velocity. In addition, the IDDI appears to be tightly correlated according to a linear relation with the mean logarithm of the emission fluxes issuing from the simulations. These results must be considered as an intervalidation between the dust production scheme and the IDDI: on one hand they demonstrate the ability of the scheme to retrieve both the frequencies and intensity of the dust events with a high confidence level; on the other hand they confirm the potential for the IDDI to constitute a quantitative measurement of the atmospheric dust loading in situations of emission.

Prospects come out of these results. Especially, the description of the overall cycle of the Saharan dust becomes feasible with an expected satisfactory degree of accuracy, in so far the major difficulties, lying in the stage of emission, are overcome. This can be realized by simulating an observed dust event, including emission, transport and deposition, and checking its description with satellite observation.

Extending the previous results on a global scale could result in an accurate description of the mineral aerosol cycle by mean of Global Circulation Models. The main difficulty to be cleared up is the adequate documentation of the dust-emitting surfaces, a task for which the use of remote sensing would certainly be convenient.

In the field of aerosol remote sensing, it appears that the IDDI is suitable to provide a quantitative estimate of the atmospheric dust content. Such an opportunity should be seized in order to assess the mass fluxes of emitted- and likely transported- desert dust.

7. ACKNOWLEDGEMENTS

This work has been supported by the "Programme Environnement du CNRS" in the framework of the action "Erosion Eolienne en Régions Arides et Semi-arides".

8. REFERENCES

1. M.O. Andreae, "Climate effects of changing atmospheric aerosol levels", *World Survey of Climatology, Vol. XX, Future Climate of the World,* A. Henderson-Sellers Ed., 1994.

2. J.R. Petit, M. Briat and A. Royer, "Ice age aerosol content from Antarctic ice core samples and past wind strength", *Nature,* vol. 293, pp. 391-394, 1981.

3. M. Sarnthein and B. Koopman, "Late Quaternary deep-sea record on Northwest African dust supply and wind circulation", *Paleoecol. of Africa,* vol. 12, pp. 239-253, 1980.

4. K. Pye and H. Tsoar, "The mechanics and geological implications of dust transport and deposition in deserts, with particular reference to loess formation and dune sand diagenesis in the northern Negev, Israel", *Deserts Sediments Ancient and Modern,* I. Reid and L. Frostick Eds., Blackwell, Oxford, 1987.

5. N.J. Middleton, "Effect on drought on dust production in the Sahel", *Nature,* vol. 316, pp. 431-434, 1985.

6. G.M. N'tchayi, J. Bertrand, M. Legrand and J. Baudet, "Temporal and spatial variations of the atmospheric dust loading throughout West Africa over the last thirty years", *Ann. Geophysic.,* vol. 12, pp. 265-273, 1994.

7. S. Jousseaume, "Three-dimensional simulations of the atmospheric cycle of desert dust particles using a general circulation model", *J. Geophys. Res.,* vol. 95, pp. 1909-1941, 1990.

8. C. Genthon, "Simulations of desert dust and sea-salt aerosols in Antarctica with a general circulation model of the atmosphere", *Tellus,* vol. 44B, pp. 371-389, 1992.

9. I. Tegen and I. Fung, "Modeling of mineral dust in the atmosphere: sources, transport and optical thichness", *J. Geophys. Res.,* vol. 99, pp. 22897-22914, 1994.

10. B. Marticorena and G. Bergametti, "Modeling the atmospheric dust cycle: 1. Design of a soil-derived dust emission scheme", *J. Geophys. Res.*, in press.

11. C. N'doumé, "Traitement de l'imagerie Météosat IR pour l'observation des aérosols désertiques au-dessus de l'Afrique: optimisation, validation et application à l'établissement des distributions spatio-temporelles", *Thèse de Doctorat,* Univ. de Lille-1, 218 pp., 1993.

12. M. Legrand, C. N'doumé and I. Jankowiak, "Satellite-derived climatology of the Saharan aerosol", *Passive Infrared Remote Sensing of Clouds and the Atmosphere II: proc. SPIE 2309,* D.K. Lynch Ed., pp. 127-135, 1994.

13. J.D. Iversen and B.R. White, "Saltation threshold on Earth, Mars and Venus", *Sedimentology,* vol. 29, pp. 111-119, 1982.

14. S.P.S. Arya, "A drag partition theory for determining the large-scale roughness parameter and wind stress on Arctic pack ice", *J. Geophys. Res.*, vol. 80, pp. 3447-3454, 1975.

15. W.P. Elliot, "The growth of the atmospheric internal boundary layer", *Eos Trans. AGU,* vol. 39, pp. 1018-1054, 1958.

16. J.K. Marshall, "Drag measurements in roughness arrays of varying density and distribution", *Agric. Meteorol.*, vol. 8, pp. 269-292, 1971.

17. Y. Shao, M.R. Raupach and P.A. Findlater, "Effect of saltation bombardment on the entrainment of dust by wind", *J. Geophys. Res.*,vol. 98, pp. 12719-12726, 1993.

18. B.R. White, "Soil transport by winds on Mars", *J. Geophys. Res.*, vol. 84, pp. 4643-4651, 1979.

19. R. Greeley, D.G. Blumberg and S.H. Williams, "Field measurements of active windblown sand", *Abstract of the Workshop on Response of Aeolian Processes to Global Change,* edited by the Desert Reaserch Institute, Occasional Paper N°2, Reno, Nevada, 1994.

20. D.A. Gillette, "Environmental factors affecting dust emission by wind erosion", *Saharan Dust,* C. Morales Ed., pp. 71-94, Wiley and Sons, New-York, 1979.

21. D.A. Gillette, J. Adams, D.R. Muhrs and R. Khil, "Threshold friction velocities and rupture moduli for crusted desert soils for the input of soil particles into the air", *J. Geophys. Res.*, vol. 87, pp. 9003-9015, 1982.

22. W.G. Nickling and J.A. Gillies, "Emission of fine-grained particulates from desert soils", *Paleoclimatology and Paleometeorology: Modern and Past Patterns of global Atmospheric Transport,* M. Leinen and M. Sarnthein Eds., pp.133-165, Kluwer Academic Publ., Dordrecht, 1989.

23. G. Williams, "Some aspects of the aeolian saltation load", *Sedimentology,* vol. 3, pp. 253-256, 1964.

24. M. Sörensen, "Estimation of some aeolian saltation transport parameters from transport rate profiles", *Proc. of the International Workshop on the Physics of Blown Sand,* O.E. Barndorff-Nielsen, J.T. Möller, K. Römer Rasmussen and B.B. Willets Eds., pp.141-190, Univ. of Aarhus, Aarhus Denmark, 1985.

25. B. Marticorena, "Modélisation de la production d'aérosols désertiques en régions arides et semi-arides: développement et validation d'un code de calcul adapté au transport à grande échelle",*Thèse de Doctorat,* Univ. Paris VII, 268 pp., 1995.

26. C.H.B. Priestley, *Turbulent Transfer in the Lower Atmosphere,* 130 pp., Univ. of Chicago Press, Chicago, 1959.

27. M.R. Raupach "Saltation layers, vegetation canopies and roughness lenghts", *Acta Mechanica,* 1(suppl.), , pp. 83-96, 1991.

28. Y. Callot, "Géomorphologie et paléoenvironnements de l'Atlas Saharien au Grand Erg Occidental: dynamique éolienne et paléolacs holocènes", *Thèse de Doctorat ès Sciences,* Univ. Paris-6, 412 pp., 1987.

29. Y. Callot and M. Fontugne, "Les étagements de nappes dans les paléolacs holocènes du nord-est du Grand Erg Occidental (Algérie)", *C.R. Acad. Sci. Paris,* vol. 315, série II, pp. 471-477, 1992.

30. B. Chatenet, B. Marticorena, L. Gomes and G. Bergametti, "Assessing the actual grain-size distribution of desert soils erodible by wind", *Sedimentology,* in press.

31. M. Legrand, J.J. Bertrand, M. Desbois, L. Ménenger and Y. Fouquart, "The potential of infrared satellite data for the retrieval of Saharan dust optical depth over Africa", *J. Appl. Meteorol.*, vol. 31, pp. 309-318, 1989.

32. D. Tanré and M. Legrand, "On the satellite retrieval of Saharan optical thickness over land: two different approaches", *J. Geophys. Res.*, vol. 96, pp. 5221-5227, 1991.

33. M. Legrand, G. Cautenet and J.C. Buriez, "Thermal impact of Saharan dust over land. Part II: Application to satellite IR remote sensing", *J. Appl. Meteorol.*, vol. 31, pp. 181-193, 1992.

34. A. Plana-Fattori, "Simulation de l'impact de l'aérosol désertique sur les températures de surface du sol et sur les luminances émergentes de la planète dans la reegion spectrale 10,5-12,5 microns. Application à l'interpretation de l'imagerie Météosat-IR", *Thèse de doctorat,* Univ. de Lille-1, T1, 245 pp.; T2, 112 pp., 1994.